Fitting a Model to Floating Gate Prompt Charge Loss Test Data for the Samsung 8 Gb SLC NAND Flash Memory

L. D. Edmonds, F. Irom, and G. R. Allen, *Member IEEE*

***Abstract*--** A recent model provides risk estimates for the deprogramming, of initially programmed floating gates, via prompt charge loss produced by an ionizing radiation environment. The environment can be a mixture of electrons, protons, and heavy ions. The model requires several input parameters. Parameters intended to produce conservative risk estimates for the Samsung 8 Gb SLC NAND flash memory are given, subject to some qualifications.

I. Introduction

The Samsung 8 Gb single-level cell (SLC) NAND flash memory is being considered for use on NASA's planned Europa mission. The total number of floating gate (FG) core memory bits in this device is approximately 8.6×10^9. One reason for this choice of devices is its hardness to total ionizing dose (TID). This is important because an extremely large dose from electrons trapped in a planetary radiation belt is anticipated for this mission (more than 1 Mrad through thin spacecraft shielding, and large enough to be a concern for any shielding). Given that TID requirements are satisfied, we still have a concern regarding single-event effects (SEE). These are produced by a single highly-ionizing particle originating from anywhere (often from galactic cosmic rays or solar particle events) that creates enough disruption in a microelectronic device to be a problem. For the older-generation flash memory devices, SEE concerns were important only in the control circuitry. But for some of the newer devices, such as the one considered here, the charge stored in an FG can be small enough to be disrupted by a single particle hit. Previous testing (discussed later in this paper) on the Samsung 8 Gb SLC NAND flash memory indicates that this device is one of those in which FG charge loss is a concern.

The topic of this paper is a prompt (i.e., occurs immediately after an ion hit) effective charge loss of the FG. The term "prompt" distinguishes this charge loss from a charge loss from a small leakage current that persists over an extended time [1]. The term "effective" is used here because there are at least two physical mechanisms that contribute to a prompt charge loss. One is an actual charge loss discussed by Cellere *et al*. [2]. The other is a partial compensation of the FG charge by charge created in a nearby oxide which was discussed by Guertin *et al.* [3]. The charge state of an FG is experimentally determined by the threshold voltage of a field-effect transistor (FET) surrounding the FG, but a voltage shift cannot distinguish an actual charge loss from charge compensation[1], so an effective charge loss refers in this paper to any combination of actual loss and compensation that produces a shift in the threshold voltage. The goal is to fit the model derived in [4] to test data for the Samsung 8 Gb SLC NAND flash memory so that the risk of the device becoming deprogrammed by the space radiation environment can be estimated.

II. The Model

Radiation-induced FG charge loss is neither the classic SEE problem nor the classic TID problem. Unlike the classic SEE problem, FG charge loss accumulates when there are multiple hits to an FG by ionizing particles. Unlike the classic TID problem, the number of hits needed to corrupt stored data can be small enough to require a statistical treatment, as opposed to approximating this number by a statistical average. The problem considered here is better described as a micro-dose problem and a model was derived in [4] for this application. Mathematical details and numerical routines are given in [4]. A brief overview of the model is given below.

The model includes two kinds of interactions. The "strong interaction" occurs when an ionizing particle directly hits an FG and produces an actual FG charge loss. The "weak interaction" occurs when an ionizing particle hits the vicinity of an FG and produces a partial compensation of the FG charge by charge created in a nearby oxide. The weak interactions are much more frequent than strong interactions (as seen by comparing interaction cross sections discussed later) but multiple weak interactions are needed to produce the same effective charge loss as one strong interaction. The model defines a charge-loss event (CLE) to be a user-defined event characterized by the charge stored in an FG crossing some threshold value via prompt charge loss. The critical

Manuscript received September 17, 2016. The research in this paper was carried out at the Jet Propulsion Laboratory, California Institute of Technology, under contract with the National Aeronautics and Space Administration (NASA). Copyright 2016 California Institute of Technology. Government sponsorship acknowledged.

Larry D. Edmonds is with the Jet Propulsion Laboratory, California Institute of Technology Pasadena, CA 91109 (telephone: 818-720-6660, e-mail: Larry.d.edmonds@jpl.nasa.gov

Farokh Irom is with the Jet Propulsion Laboratory, California Institute of Technology Pasadena, CA 91109 (telephone: 818-354-7463, e-mail: Farokh.irom@jpl.nasa.gov

Gregory R. Allen is with the Jet Propulsion Laboratory, California Institute of Technology Pasadena, CA 91109 (telephone: 818-393-7558, e-mail: Gregory.r.allen@jpl.nasa.gov

Reference herein to any specific commercial product, process, or service by trade name, trademark, manufacturer, or otherwise, does not constitute or imply its endorsement by the United States government or the Jet Propulsion Laboratory, California Institute of Technology. © 2016 California Institute of Technology. Government sponsorship acknowledged.

[1] Sometimes a distinction can be made by investigating the time profile of the voltage shift [3], but the analysis given here will not require such measurements.

charge loss is the amount of charge an FG must lose (effective charge loss will always be assumed when not explicitly clarified) to produce a CLE. In the context of this work, a CLE will be the deprogramming of an initially programmed (charged) FG in a flash memory, and the critical charge loss is the amount of charge an FG must lose to be sensed as deprogrammed. There is a statistical distribution of critical charge losses because there is a statistical distribution of initial FG charges during programming.

The model in [4] combines three kinds of statistics. The first (strong interactions) and second (weak interactions) both refer to charge losses produced by an ion hit. These statistics depend on the environment. The third statistic, critical charge loss, is a device characteristic independent of the environment.

The model begins with six fitting parameters but then reduces this number to five. One of the original fitting parameters, denoted a_1, is defined by the condition that the charge loss from one strong interaction produced by a normal-incident heavy ion is the ion LET divided by a_1. Another parameter, denoted σ_S here, is the cross section per FG for a strong interaction. Two other parameters, denoted a_2 and σ_W, have the same interpretations for weak interactions that a_1 and σ_S have for strong interactions. The last two of the six parameters describe the statistical distribution of critical charge losses. This distribution is described by a Weibull function with shape parameter k and scale parameter λ. However, the parameters a_1, a_2, and λ appear in the analysis in [4] only in two combinations. One combination is $a_1\lambda$ and the other is $a_2\lambda$. Therefore if we define the b-parameters by $b_1 \equiv a_1\lambda$ and $b_2 \equiv a_2\lambda$, then there are only five independent fitting parameters, which are b_1, b_2, σ_S, σ_W, and k. The parameter b_1 is a measure of the sensitivity of an FG to strong interactions, with smaller values of b_1 implying greater sensitivity in the sense that a smaller LET is needed to produce a CLE, while σ_S is proportional to the frequency of occurrence of strong interactions in a fixed radiation environment. The parameters b_2 and σ_W have the same interpretations for weak interactions that b_1 and σ_S have for strong interactions. These are the parameters used by the model in [4] except for a small change in notation where $\sigma_{S,sat}$ and $\sigma_{W,sat}$ in [4] replace the σ_S and σ_W used here. Note that σ_S is expected to be roughly equal to the physical area of the FG because a direct hit to the FG is needed for a strong interaction, but σ_W has a more obscure geometric interpretation. The parameter k is a measure of the amount of spread in the statistical distribution of critical charge loss. A large value of k describes a small amount of FG-to-FG variation in the critical charge loss (the cumulative Weibull function becomes a step function in the large-k limit) while smaller values describe more spread in the distribution.

III. Small-Fluence Data

A collection of FGs (e.g., a flash memory device) exhibits SEU-like behavior when nearly all FGs that underwent a CLE received only one ion hit. This can be recognized in heavy-ion test data by the number of CLE counts being proportional to fluence. Given that the LET is large enough so that counts can be produced by single hits, this behavior can still only occur when the fluence is sufficiently small, so this behavior is also known as "small-fluence" behavior. The phrases "SEU-like" behavior and "small-fluence" behavior are used interchangeably in this paper. Although weak interactions are much more frequent than strong interactions within the general FG population, the unlucky subset of FGs that exhibited a CLE under small-fluence conditions is the small and unlucky population of FGs that experienced a strong interaction. Furthermore, very few of these had significant charge loss from weak interactions because the small-fluence condition implies that a small fraction of the general FG population experienced weak interactions, and this also applies to the subset of FGs that experienced a strong interaction. Therefore, measured data under small-fluence conditions do not provide any information regarding weak interactions.[2] Furthermore, such data do not provide any tests of the assertion that charge loss accumulates over multiple ion hits. However, such data do provide information regarding the strong interactions. Furthermore, such data have the convenient property that CLE cross sections can be defined because CLE counts are proportional to fluence. For any device (such as the Samsung 8 Gb SLC NAND flash memory) in which the FG area is on the order of 0.1 µm × 0.1 µm (or 10^{-10} cm^2), the heavy-ion fluences typically used for SEE testing (between 10^6 and 10^7/cm^2) qualify as small-fluence conditions.

The set of points in Fig. 1 (the curves will be discussed later in Section V) is a compilation of small-fluence CLE cross section data for the Samsung 8 Gb SLC NAND flash memory, but with LET converted from Si to SiO_2 as recommended in [4]. (This LET conversion is not very significant for this data set.) The CLE cross section is experimentally defined to be the number of CLE counts divided by fluence. It is divided again by the number of FGs in the device (a.k.a., the number of memory bits) when presented as a per-FG cross section, as it is in Fig. 1. The points labeled TAM 1 are from the first (out of two) tests performed at the TAM facility and the data were previously reported in [5]. The points labeled RADEF are from tests performed at the RADEF facility and the data were first reported in [6] but can also be found in [5]. The TAM 2 points were not previously published and these data are presented for the first time in this paper in the next section.

IV. Large-Fluence Data

As pointed out in the previous section, the small-fluence data represented in Fig. 1 do not provide any information regarding weak interactions, or any tests of the assertion that charge loss accumulates over multiple ion hits. Large-fluence (meaning that the fluence is large enough to violate SEU-like behavior, i.e., the number of counts is not proportional to fluence) data are needed for this. It might be argued that a laboratory fluence should not be required to exceed an application fluence by more orders-of-magnitude than needed to obtain the statistical significance required for a risk estimate. But a counter-argument points out that if an

[2] This statement is sometimes (perhaps usually) correct but not always. It will be argued in Section VI that weak interactions can affect the saturation SEU cross section for those cases in which the critical charge loss is very small.

application radiation environment is different than the laboratory environment, a device must be completely characterized in order to use test data to make predictions for the application environment. In particular, if weak interactions and/or the additive effect from multiple hits are possible concerns for an application environment, a more complete characterization is needed. This motivated an additional test (the TAM 2 test) of the Samsung 8 Gb SLC NAND flash memory. Earlier work by Guertin *et al*. [3] was the first to recognize cumulative effects when interpreting large-fluence data and the goal here is to obtain similar data for the Samsung 8 Gb SLC NAND flash memory. Specifically, the goal is to test with fluences large enough to make weak interactions, and the additive property of charge loss, to become observable in the data.

The choice of test ions follows recommendations in [4]. Specifically, we look for a test ion that satisfies two conditions. One condition is that scatter in the data associated with counting statistics (i.e., Poisson error bars) is tolerable, so we do not want the LET to be small enough to make the number of counts too small. This condition becomes a constraint when combined with a more practical consideration that beam runs become a problem when fluences are greater than 10^9/cm^2. The other condition discussed in [4] is that the LET, denoted L, produces a large value for the ratio $\sigma_{CLE}(2L)/\sigma_{CLE}(L)$, where σ_{CLE} is the small-fluence CLE cross section discussed in the previous section. Based on these considerations together with the TAM 1 and RADEF data in Fig. 1, we judged that an informative data set could be provided by the TAM facilities using two ions. One is Ar out of the beam, which is 15 MeV/amu before penetrating the air gap and device over-layers, but becomes degraded by the air gap and over-layers to an energy of about 520 MeV and produces an LET in SiO_2 of about 9.0 MeV-cm^2/mg (or an LET in Si of about 8.3 MeV-cm^2/mg). The other selected ion was Ne but with an energy degrader selected to produce an energy of 150 MeV at the location of interest, so the LET is 4.55 in SiO_2 (or 4.2 MeV-cm^2/mg in Si).

The experimental arrangement for the TAM 2 test is briefly described as follows.

The SEE heavy ion measurements were performed on the commercial SLC 8Gb NAND flash memory manufactured by Samsung. The part number is K9F8G08U0M and the date code is 1031-CMF320PV. SEE measurements were taken using a commercial memory tester called SIGNAS-II. The SIGNAS-II consists of a motherboard with an FPGA (Altera Cyclone III); a daughter board with TSOP socket for NAND; and Windows-based analysis software. The maximum operating frequency of the SIGNAS-II is 20MHz cycle time, which is the operating frequency used during the measurements. During the SEE measurements, V_{cc} was set to 3.3 V. Note that the Ne ions were degraded for TAM2 data, but not TAM1 data. The SEE tests were conducted by first loading all 8Gb of the DUT with an all all-zeros pattern (which puts the FGs in a charged state) and then verifying the pattern by reading it back from the device. Measurements were performed in static mode. A series of irradiations were performed to accumulate total fluence of 1×10^6, 2×10^6, 5×10^6, 1×10^7, 2×10^7, 5×10^7, 1×10^8, 2×10^8, 5×10^8 and 1×10^9 /cm^2 for each ion. After irradiation, the device's power was cycled, the device was read again, checked for errors, and logged. This final check after a power cycle reveals errors that are from bit upsets in the floating gates. We didn't perform any program/erase operations on the device after each irradiation step.

The data obtained from the TAM 2 test are shown as the points in Fig. 2 (the curves are discussed in the next section). A fluence of 10^7/cm^2 qualifies as a small-fluence condition (i.e., produces SEU-like behavior) so the counts at this fluence were used to obtain the two TAM 2 cross section points in Fig. 1.

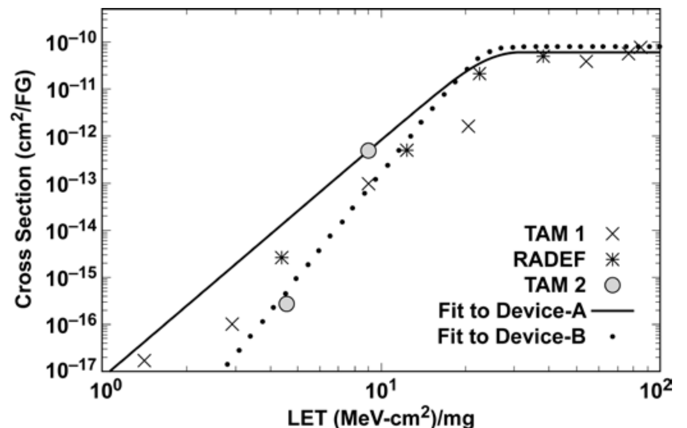

Fig. 1: Small-fluence (a.k.a., SEU-like) cross sections versus LET for the Samsung 8 Gb SLC NAND flash memory. The TAM 2 points are new data reported in this paper. All other points were obtained from prior publications. The solid curve is a fit to a more complete set of data (see Fig. 2) for one device and the dotted curve is a fit to a more complete set of data for a different device.

TABLE I: FITTING PARAMETERS USED TO CONSTRUCT THE CURVES IN FIGS. 1 AND 2

Device	b_1 (MeV-cm^2/mg)	b_2 (MeV-cm^2/mg)	$\sigma_{S,sat}$ (cm^2)	$\sigma_{W,sat}$ (cm^2)	k
A	23.2	1155	6.00×10^{-11}	1.00×10^{-8}	5.057
B	22.8	2271	7.74×10^{-11}	2.00×10^{-9}	7.419

V. Fits to Data

One observation from Fig. 1 is that there is a considerable amount of part-to-part variations. It is therefore best to assign to each device its own unique set of fitting parameters. Fortunately, this is possible for the two parts in TAM2 that produced the data in Fig. 2 because each data set provides a complete characterization. The part that was tested with Ar will be called Device A, and the one tested with Ne will be called Device B.[3] The numerical routines in [4] were used for

[3] In retrospect it is now clear that several parts should have been tested with the same ion during the TAM 2 tests so that part-to-part variations could have been assessed without the additional complication of different parts being tested with different ions. This was not done because the severity of part-to-part variations was not recognized at the time the test plan was being worked out. It is recommended that this be done for future tests.

separate fits to each data set and the fits are shown as the curves in Fig. 2, with fitting parameters given in Table I. That the best fit does not conform as closely to the data for Ne as for Ar is understandable because larger Poisson error bars accompany the smaller numbers of counts produced by Ne (error bars need not be shown in Fig. 2 because they are implied by the numbers of counts).

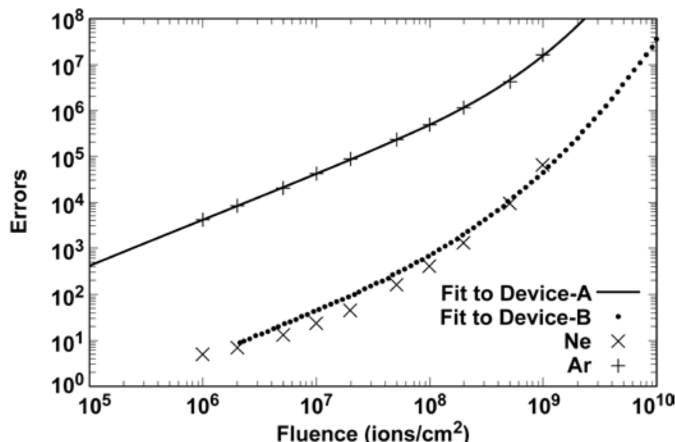

Fig. 2. Large-fluence data expressed as the number of counts versus fluence for the Samsung 8 Gb SLC NAND flash memory. The points are from the TAM 2 tests. The solid curve is a fit to the Ar points alone because a different device produced the Ne data. The dotted curve is a fit to the Ne data alone.

Comparing parameters for the two devices in Table I reveals similarities and differences. The two devices are similar regarding their sensitivity (measured by b_1) and cross section (σ_S) for strong interactions (model sensitivity to these parameters is such that there is little distinction between the two devices with regards to these parameters). This might seem reasonable if we assume that these parameters are primarily controlled by the masking portion of device fabrication, which is done with tight tolerances with little part-to-part variations. However, the two devices are significantly different with regards to weak interactions (b_2 and σ_W). This might seem reasonable if we assume that weak interactions are produced by the charging of nearby oxides because considerable part-to-part variations are often seen in TID test data (hence TID testing is typically performed on several parts) due to the fact that TID sensitivity is affected by a variety of processing variables during device fabrication. A second difference between the parts represented by Table I is not unreasonable but perhaps also not anticipated. This is in the parameter k. The model is sensitive enough to this parameter to make the two values in Table I significantly different. As pointed out in Section II, the parameter k measures the spread in the statistical distribution of threshold voltages with smaller values of k indicating a greater spread. We see from Table I that Device-B has the larger k and therefore a tighter distribution of threshold voltages. This is consistent with Fig. 1 showing that the cross section versus LET curve has a steeper slope for Device-B than for Device-A (the parameter k determines the slope seen in a log-log plot of small-fluence cross section versus LET).

VI. Including TID

A device response to ionizing particles is called dose-like if the particles are so lightly ionizing that the number of particle hits needed to produce an observable effect is large enough to be approximately deterministic, i.e., can be approximated by the statistical average number of hits. The model in [4] includes the case in which a dose-like environment (e.g., electrons trapped in a planetary radiation belt) is added to a heavy-ion environment. The dose-like environment is input to the model by specifying a TID level while the heavy-ion environment is described in terms of fluence at each relevant LET. An example irradiation history for which the model was intended to apply is discussed in [5]. Several devices were exposed to γ-rays from a ^{60}Co source prior to (and without erase or programming operations) performing heavy-ion tests. The heavy-ion tests (SEU tests) are small-fluence tests for which CLE cross sections can be defined, and these cross sections are reported in [5] for the Samsung 8 Gb SLC NAND flash memory for each of several TID levels produced by the ^{60}Co exposures.

Unfortunately, the model in [4] has a limitation. The model was derived under the assumption that the only effect from the dose-like environment is to produce an FG charge loss, with the control circuitry being unaffected by TID.[4] However, there appears to be a significant TID effect in the control circuitry for those devices discussed in [5] that were exposed to TID before performing the SEU tests. This conclusion was reached by considering the bias dependence of the device response to TID when the bias is applied during the TID exposure. This consideration is relevant because Cellere *et al*. [8] argued that FG charge loss should not have a strong bias dependence because the dielectrics surrounding the FGs are too thin for carrier recombination to be important. Therefore a strong bias dependence indicates TID effects in the control circuitry. We now specifically consider the devices discussed in [5] that were exposed to TID before performing the SEU tests. According to the test log for the data discussed here, three devices initially programmed in an all-zero (charged) bit pattern were exposed to 150 krad(Si) while unbiased and then the CLEs were counted before (as well as after) performing the heavy-ion tests. The numbers of counts prior to SEU testing, i.e., from TID alone, were between 1×10^4 and 2.1×10^4 for each of the three devices. Another set of two devices were investigated in the same way except that they were biased during TID exposure. The counts for those devices were between 4.5×10^8 and 4.9×10^8 for each of the two. We see that the device response to TID is strongly dependent on bias conditions during TID exposure, indicating that the control circuits were affected by TID. We can also conclude that the charge-sensing portion of the control circuit is affected by

[4] The relative importance of TID in the FG compared to TID in the control circuitry is greatest for the most granular forms of radiation (e.g., heavy ions compared to γ-rays). This is because CLEs reflect the FGs that underwent the maximum charge loss and the more granular forms of radiation produce the larger ratios of maximum charge loss to average (over the entire FG population) charge loss.

TID because the initial programming was done before the TID exposure.

It was concluded above that there is a significant TID effect in the control circuitry for those samples of the Samsung 8 Gb SLC NAND flash memory discussed in [5] that were exposed to TID before performing the SEU tests. A TID effect in the control circuitry effectively changes the device into a different device. Proper use of the model in [4] for this case would have a separate row in Table I for each TID level. However, if our primary goal is to merely obtain a correct (or conservative if not correct) prediction from the model, we can do this using pre-TID fitting parameters if we include one more fitting parameter. This is a dose-enhancement factor (DEF). First consider the DEF that has a physical definition and is relevant when material structures of interest are too thin for charged particle equilibrium to apply [7]. Dose typically reported as a measure of a radiation environment (denoted $D_{reported}$) is an equilibrium absorbed dose, which is the dose in materials thick enough for charged particle equilibrium to apply. The DEF is defined by

$$D = \text{DEF} \times D_{reported} \tag{1}$$

where D is the local dose in a thin material that might be adjacent to dissimilar materials. The DEF as a physically defined quantity is not expected to be greater than 2 when TID is from a ^{60}Co source with low-energy photons filtered out [7], [9]. Now consider the DEF as a model fitting parameter. This also satisfies (1) except that the D in (1) is now the model input needed for the model to give a correct prediction. The DEF as a model fitting parameter must do more than convert equilibrium dose into local dose. It must also compensate (in the sense of making a model prediction agree with data) for the use of pre-TID parameters when post-TID parameters are more appropriate. Therefore the DEF as a model fitting parameter can be larger than the physically-defined DEF.

To determine the DEF as a model fitting parameter, we consider the data in [5] pertaining to devices exposed to TID (from a ^{60}Co source) prior to (and without any erase or programming operations) performing heavy-ion SEU tests. The SEU tests were done with three ions; Xe (with LET of 51.5 MeV-cm^2/mg in Si, or 54 MeV-cm^2/mg in SiO_2), Ar (with LET of 8.3 MeV-cm^2/mg in Si, or 9.0 MeV-cm^2/mg in SiO_2), and Ne (with LET of 2.7 MeV-cm^2/mg in Si, or 2.9 MeV-cm^2/mg in SiO_2). SEU data from parts without prior TID were already included in the TAM 1 data set in Fig. 1 so here we focus on devices with prior TID. We consulted the test log for details not reported in [5] and obtained the following information. The Xe cross sections for the pre-TID of 100 krad(Si) are averaged over two devices but the part-to-part variation was not significant. Similarly, the Xe cross sections for the pre-TID of 150 krad(Si) are averaged over two devices but the part-to-part variation was again not significant. The fluence used for each of these data points was 2×10^6/cm^2, which qualifies as a small-fluence test condition. The Ar test with a pre-TID of 100 krad(Si) and the Ar test with a pre-TID of 150 krad(Si) were each performed on one device using a fluence of 5×10^6/cm^2, which qualifies as a small-fluence test condition. The Ne test was performed only with a pre-TID of 150 krad(Si) and was performed on one device but the fluence was 2×10^8/cm^2, which does not qualify as a small-fluence test condition. In fact, the Ne cross section for a pre-TID of 150 krad(Si) is clearly a mismatch with the Ar cross section for a pre-TID of 150 krad(Si). The Ne cross section is 6.70×10^{-11} cm^2 at an LET (in SiO_2) of 2.9 MeV-cm^2/mg, compared to the smaller Ar cross section of 1.79×10^{-11} cm^2 at the larger LET of 9.0 MeV-cm^2/mg. The obvious explanation for this mismatch is that the Ne tests were not small-fluence tests. We therefore include only the Xe and Ar points, and these are shown as the points identified as 100 krad and 150 krad in Fig. 3. All other points in Fig. 3 are from Fig. 1. The curves in Fig. 3 are discussed below.

The curves in Fig. 3 are model predictions using (1) together with the parameters in Table II. The upper curve represents $D_{reported}$ = 150 krad(Si), the middle curve represents $D_{reported}$ = 100 krad(Si), and the lower curve represents $D_{reported}$ = 0. The parameters in Table II were selected for a conservative representation of the data. The parameters were obtained by starting with the Device A fitting parameters in Table I (which produce more conservative predictions than the Device B parameters) and then adjusting σ_S. This adjustment was motivated by the fact that the data in Fig. 3 show a larger saturation cross section for the devices exposed to TID compared to the others. The probable explanation is that the TID further weakened the subset of FGs that were already weak to the point that one weak interaction from a heavy ion with a very large LET is enough to produce a count. Although the most general form of the model in [4] (including the application that produced the curves in Fig. 2) includes weak interactions from heavy ions, the SEU-limit of the model does not and therefore cannot agree with the larger saturation cross section produced by TID unless σ_S is modified. To be conservative, σ_S was adjusted to agree with the saturation cross section for the 150 krad(Si) data, even though this causes the model predictions to overestimate the saturation cross section for the other data sets. This explains the first five parameters in Table II. Finally, DEF was selected to agree with the Ar data point at 150 krad(Si) in Fig. 3.

The DEF in Table II, which produces agreement with 150 krad(Si) data when the TID source is ^{60}Co, is expected to be a conservative estimate of the DEF applicable to 150 krad(Si) when the TID source is radiation belt electrons. This conclusion is based on the observation reported in [5] that a given dose from electrons has a smaller effect on the device than the same amount of dose from a ^{60}Co source. The observation reported in [5] referred to 60 MeV electrons but we assume here that the conclusion will also be true for an electron spectrum found in space. Conservatism for 150 krad(Si) of electrons combined with the conservatism in model predictions seen in Fig. 3 for all other data points

means that model predictions will be conservative for electron doses less than or equal to 150 krad(Si). However, the DEF given here is a model input parameter, not a physically-defined quantity, because it includes an empirical correction for TID effects in the control circuitry. This DEF was not derived from any physical analysis. It was selected to produce conservative predictions for doses up to 150 krad(Si). Model predictions using the Table II parameters cannot be assumed to be conservative for doses (from any source) in excess of 150 krad(Si).

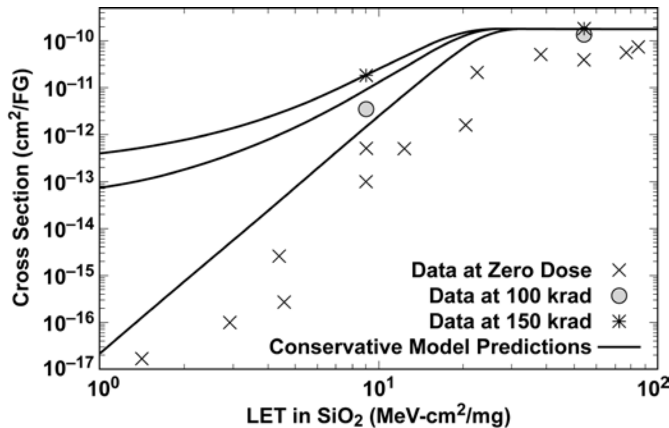

Fig. 3: Cross sections versus LET for the 8 Gb SLC NAND flash memory after several levels of TID exposure. The points at zero dose are from Fig. 1. The curves are model predictions using the parameters in Table II. The upper curve refers to 150 krad(Si), the middle curve refers to 100 krad(Si), and the lower curve refers to zero dose.

TABLE I: PARAMETERS FOR CONSERVATIVE PREDICTIONS

b_1 (MeV-cm^2/mg)	b_2 (MeV-cm^2/mg)	$\sigma_{S,sat}$ (cm^2)	$\sigma_{W,sat}$ (cm^2)	k	DEF
23.2	1155	1.80×10^{-10}	1.00×10^{-8}	5.057	1.65

VII. CONCLUSION

The model in [4] provides risk estimates for the deprogramming of initially programmed FGs via prompt charge loss produced by an ionizing radiation environment. The environment can be a mixture of radiation belt electrons (described in terms of dose) and heavy ions (described in terms of fluence as a function of LET). The model requires several input parameters. Parameters intended to produce conservative (providing that the programming is done before TID exposure) risk estimates for the Samsung 8 Gb SLC NAND flash memory are given in Table II. The estimates are expected to conservative for electron doses up to 150 krad(Si) but cannot be assumed to be conservative at larger doses. The parameters b_1, b_2, σ_S, σ_W, and k are entered directly into the model in [4] (except for a change in notation with σ_S and σ_W denoted $\sigma_{S,sat}$ and $\sigma_{W,sat}$ in [4]). The parameter DEF is used to calculate D via (1) and then D is entered into the model. The DEF in Table II includes an empirical correction to account for TID effects in the charge-sensing circuits and was selected to produce conservative estimates for doses up to 150 krad(Si).

ACKNOWLEDGEMENT

The authors would like to thank Steven M. Guertin, Charles E. Barnes, and Leif Z. Scheick of JPL for helpful suggestions.

REFERENCES

[1] A. Scarpa, A. Paccagnella, F. Montera, G. Ghibaudo, G. Pananakakis, G. Ghidini, and P. G. Fuochi, “Ionizing radiation induced leakage current on ultra-thin gate oxides,” *IEEE Trans. Nucl. Sci.*, vol. 44, no. 6, pp. 1818-1825, Dec. 1997.

[2] G. Cellere, A. Paccagnella, A. Visconti, M. Bonanomi, and A. Candelon, “Transient conductive path induced by a single ion in 10 nm SiO2 layers,” *IEEE Trans. Nucl. Sci.*, vol. 51, no. 6, pp. 3304-3311, Dec. 2004.

[3] S. M. Guertin, D. N. Nguyen, and J. D. Patterson, “Microdose induced data loss on floating gate memories,” *IEEE Trans. Nucl. Sci.*, vol. 53, no. 6, pp. 3518-3524, Dec. 2006.

[4] L. D. Edmonds, *A Method for Estimating the Probability of Floating Gate Prompt Charge Loss in a Radiation Environment*, JPL Publication 16-9, Jet Propulsion Laboratory, March 2016 (online: https://rgdoi.net/10.13140/RG.2.1.5191.0803).

[5] F. Irom and G. R. Allen, “Heavy ion, proton and electron single-event effect measurements of NAND flash memory,” submitted for publication.

[6] F. Irom, D. N. Nguyen, R. Harboe-Sorensen, and A. Virtanen, “Evaluation of mechanisms in TID degradation and SEE susceptibility of single- and multi-level high density NAND flash memories,” *IEEE Trans. Nucl. Sci.*, vol. 58, no. 5, pp. 2477-2482, Oct. 20011.

[7] T. P. Ma and P. V. Dressendorfer (editors), *Ionizing Radiation Effects in MOS Devices and Circuits*, John Wiley and Sons, 1989.

[8] G. Cellere, A. Paccagnella, A. Visconti, M. Bonanomi, P. Caprara, and S. Lora, “A model for TID effects on floating gate memory cells,” *IEEE Trans. Nucl. Sci.*, vol. 51, no. 6, pp. 3753-3758, Dec. 2004.

[9] D. M. Long, D. G. Millward, and J. Wallace, “Dose enhancement effects in semiconductor devices,” *IEEE Trans. Nucl. Sci.*, vol. NS-29, no. 6, pp. 1980-1984, Dec. 1982.